UDC 621.313.282 https://doi.org/10.20998/2074-272X.2021.5.01

V.F. Bolyukh, I.S. Schukin, J. Lasocki

INFLUENCE OF THE INITIAL WINDING DISPLACEMENT ON THE INDICATORS OF THE ELECTROMECHANICAL INDUCTION ACCELERATOR OF CYLINDRICAL CONFIGURATION

Purpose. *The purpose of the article is to determine the influence of the initial displacement of the windings on the indicators of an electromechanical induction accelerator of a cylindrical configuration with pulsed excitation from a capacitive energy storage and with short-term excitation from an alternating voltage source.* ***Methodology.*** *To take into account the interrelated electrical, magnetic, mechanical and thermal processes, as well as a number of nonlinear dependencies, we use the lumped parameters of the windings, and the solutions of the equations describing these processes are presented in a recurrent form. The mathematical model of the accelerator takes into account the variable magnetic coupling between the windings during the excitation of the inductor winding. When calculating the parameters and characteristics of the accelerator, a cyclic algorithm is used.* ***Results.*** *At a frequency of an alternating voltage source of 50 Hz, the current amplitude in the armature winding is less than in the inductor winding. With an increase in the source frequency to 250 Hz, the phase shift between the winding currents decreases. The current in the inductor winding decreases, and in the armature winding it increases. The accelerating components of the force increase, and the braking ones decrease. With an increase in the source frequency to 500 Hz, the current density in the armature winding exceeds that in the inductor winding. In this case, the phase shift between the windings is further reduced.* ***Originality.*** *When a cylindrical accelerator is excited, the largest amplitude of the current density in the inductor winding occurs at the maximum initial displacement of the windings, but the amplitude of the current density in the armature winding is the smallest. The largest value of the current density in the armature winding occurs in the absence of an initial displacement. When excited from a capacitive energy storage, the electrodynamic force between the windings has an initial accelerating and subsequent braking components. As a result, the speed of the armature initially increases to a maximum value, but decreases towards the end of the electromagnetic process. When a cylindrical accelerator is excited from an alternating voltage source, a phase shift occurs between the currents in the windings, which leads to the appearance of alternating accelerating and decelerating components of electrodynamic forces. The accelerating components of the force prevail over the braking components, which ensures the movement of the armature.* ***Practical value.*** *At a frequency of an alternating voltage source of 50 Hz, the highest speed at the output of the accelerator v_{zf}=0.5 m/s is realized at an initial displacement of the windings z_0=6.2 mm, at a frequency of 250 Hz, the highest speed v_{zf}=2.4 m/s is realized at z_0=3.1 mm, and at a frequency of 500 Hz the highest speed v_{zf}=2.29 m/s is realized at z_0=2.3 mm.* References 19, figures 9.

Key words: **electromechanical induction accelerator, cylindrical configuration, initial winding displacement, capacitive energy storage, alternating voltage source, armature speed.**

В електромеханічному індукційному прискорювачі циліндричної конфігурації найбільша амплітуда струму в обмотці індуктора виникає при максимальному початковому зсуві, але амплітуда струму в обмотці якоря при цьому найменша. Найбільша величина струму в обмотці якоря виникає при відсутності початкового зсуву. При збудженні від ємнісного накопичувача енергії електродинамічна сила між обмотками має початкову прискорювальну і подальшу гальмівну складові. Внаслідок цього швидкість якоря спочатку зростає до максимально величини, але потім зменшується до моменту закінчення електромагнітного процесу. При збудженні прискорювача від джерела змінної напруги (ДЗН) між струмами в обмотках виникає фазовий зсув, що призводить до почергової зміни прискорювальних і гальмівних складових електродинамічної сили. Прискорювальні складові сили переважають над гальмівними складовими, що забезпечує переміщення якоря. При частоті ДЗН 50 Гц амплітуда струму в обмотці якоря менше, ніж в обмотці індуктора. Зі збільшенням частоти ДЗН фазовий зсув між струмами обмоток зменшується, струм в обмотці індуктора зменшується, а в обмотці якоря збільшується. Прискорювальні складові сили збільшуються, а гальмівні – зменшуються. При підвищенні частоти ДЗН до 500 Гц щільність струму в обмотці якоря перевищує аналогічну величину в обмотці індуктора. Бібл. 19, рис. 9.

Ключові слова: **електромеханічний індукційний прискорювач, циліндрична конфігурація, початковий зсув обмоток, ємнісний накопичувач енергії, джерело змінної напруги, швидкість якоря.**

В электромеханическом индукционном ускорителе цилиндрической конфигурации наибольшая амплитуда тока в обмотке индуктора возникает при максимальном начальном смещении, но амплитуда тока в обмотке якоря при этом наименьшая. Наибольшая величина тока в обмотке якоря возникает при отсутствии начального смещения. При возбуждении от емкостного накопителя энергии электродинамическая сила между обмотками имеет начальную ускоряющую и последующую тормозящую составляющие. Вследствие этого скорость якоря вначале возрастает до максимально величины, но затем уменьшается к моменту окончания электромагнитного процесса. При возбуждении ускорителя от источника переменного напряжения (ИПН) между токами в обмотках возникает фазовый сдвиг, приводящий к возникновению чередующихся ускоряющих и тормозящих составляющих электродинамической силы. Ускоряющие составляющие силы преобладают над тормозящими составляющими, что обеспечивает перемещение якоря. При частоте ИПН 50 Гц амплитуда тока в обмотке якоря меньше, чем в обмотке индуктора. С увеличением частоты ИПН фазовый сдвиг между токами обмоток уменьшается, ток в обмотке индуктора уменьшается, а в обмотке якоря увеличивается. Ускоряющие составляющие силы увеличиваются, а тормозящие уменьшаются. При повышении частоты ИПН до 500 Гц плотность тока в обмотке якоря превышает аналогичную величину в обмотке индуктора. Библ. 19, рис. 9.

Ключевые слова: **электромеханический индукционный ускоритель, цилиндрическая конфигурация, начальное смещение обмоток, емкостной накопитель энергии, источник переменного напряжения, скорость якоря.**

Introduction. Electromechanical induction accelerators (EIAs) provide acceleration of the actuator to a high speed in a short active section [1-5]. In these coaxial accelerators, the stationary inductor winding, excited either from a capacitive energy storage (CES) or from an alternating voltage source (AVS), induces a current in the armature winding. The interaction of the armature winding current with the magnetic field of the inductor winding leads to the emergence of an electrodynamic force. Under the action of the axial electrodynamic force, the armature winding together with the actuator move linearly relative to the inductor winding, accelerating to high speed. All electromagnetic and electromechanical processes in the EIA proceed for a short time with indicators that significantly exceed the corresponding indicators of linear electric motors with a long operating mode.

EIAs are used in many areas of science and technology. Such accelerators are used in test installations for shock loads, in high-speed electrical devices and valve-switching equipment, in launchers, etc. [6-11] for example, work [12] describes a setup for testing electronic equipment in a collision with a moving object. Launchers are also used for many classes of unmanned aerial vehicles [4, 13]. Systems of active protection of armored devices from enemy objects on the approach are being developed on the basis of EIAs [14].

Features and problems of EIAs. EIAs with axial symmetry of the windings can have a disk or cylindrical configuration. In a disk accelerator, the windings of the inductor and the armature are made in the form of relatively thin disks with similar radial dimensions. In the initial position, the disk windings are set at the minimum axial distance from each other, at which the magnetic coupling is maximum. But as the armature winding accelerates, the magnetic coupling between the windings decreases sharply [15].

In a cylindrical accelerator, the windings are made in the form of hollow cylinders, the axial dimensions of which significantly exceed the radial thickness of the windings. In such an accelerator, the armature winding can move axially inside or outside the inductor winding. This makes such a design preferable, since with a larger displacement of the armature winding, and hence a longer interaction time, an effective magnetic coupling between the windings is ensured. Figure 1 shows a diagram of an EIA of a cylindrical configuration with a fixed outer winding of the inductor 1 and an accelerated inner winding of the armature 2. As the armature winding axially displaces inside the inductor winding, the magnetic coupling, characterized by the mutual inductance M_{12} between the windings, remains at a greater distance when the armature winding moves in comparison with the disk accelerator. This makes the design of the cylindrical accelerator more promising in comparison with the disk configuration.

The armature can be made in the form of a multi-turn short-circuited winding or in the form of a massive electrically conductive element. The massive armature is structurally simpler and has increased reliability. However, the induced current in the massive armature is distributed nonuniformly over the volume, which negatively affects the electromechanical parameters of the EIA. In a tightly wound multi-turn short-circuited armature, impregnated and monolithic with epoxy resin, despite a more complex design and reduced reliability, a uniform distribution of the induced current over the volume is ensured [6]. This makes it more promising, especially for the cylindrical EIA.

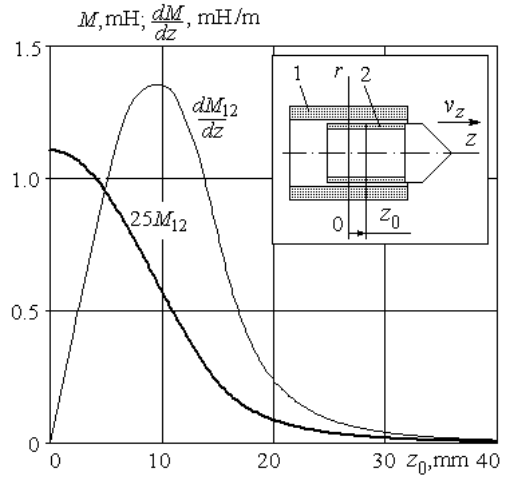

Fig. 1. Dependence of the mutual inductance between the windings M_{12} and its gradient dM_{12}/dz of the EIA on the initial displacement of the windings z_0:
1 – inductor winding; 2 – armature winding

However, in the EIA of the cylindrical configuration, the problem arises of choosing the initial displacement z_0 of the armature winding relative to the inductor winding. This is due to the fact that in the absence of the indicated displacement, when the central planes of the windings coincide, the magnetic coupling between the windings will be greatest. Accordingly, the induced current in the armature winding will be the highest. However, the axial electrodynamic force

$$f_z(t,z) = i_1(t) i_2(t) \frac{dM_{12}}{dz}(z),$$

where i_1, i_2 are the currents in the inductor and armature windings, respectively, driving the armature winding will be absent. This is due to the fact that the force f_z is proportional to the gradient of the mutual inductance in the axial direction dM_{12}/dz. As the initial displacement z_0 of the armature winding 2 increases relative to the inductor winding 1, the value of the mutual inductance M_{12} between the windings decreases, while the gradient of the mutual inductance dM_{12}/dz has a maximum at a certain value of z_0 (Fig. 1).

Since the currents in the accelerator windings flow for a short time, the question arises about the choice of the initial displacement z_0 of the armature winding 2 relative to the inductor 1 winding, at which the EIA of the cylindrical configuration provides the highest speed of the armature winding together with the actuator at the output of the accelerator v_{zf}.

The goal of the paper is to determine the influence of the initial displacement of the windings on the indicators of an electromechanical induction accelerator of a cylindrical configuration with pulsed excitation from

a capacitive energy storage and with short-term excitation from an alternating voltage source.

EIA mathematical model. Consider an electromechanical induction accelerator, in which the windings are tightly wound with round copper wire and made monolithic by impregnation with epoxy resin, followed by its hardening. To take into account the interrelated electrical, magnetic, mechanical and thermal processes, as well as a number of nonlinear dependencies, for example, of resistance on temperature, we use the lumped parameters of the windings, and the solutions of the equations describing these processes will be presented in a recurrent form [16]. The mathematical model of the EIA takes into account the changing magnetic coupling between the windings during the excitation of the inductor winding.

When calculating the parameters and characteristics of the accelerator, a cyclic algorithm is used. For this, the workflow is divided into a number of numerically small time intervals $\Delta t = t_{k+1} - t_k$ within which all quantities are considered unchanged. On the k-th cycle, using the parameters calculated at the time t_k as initial values, the parameters are calculated at the time t_{k+1}. To determine the currents over the time interval Δt, we use linear equations with unchanged parameter values. We choose a small value of the calculated step Δt so that it does not have a significant effect on the results of computer calculations, while ensuring the required accuracy.

The change in the spatial position of the armature winding is taken into account by the change in flux linkage Ψ between the windings [16]:

$$\frac{d\Psi}{dt} = M_{12}(z)\frac{di_n}{dt} + v_z(t)i_n\frac{dM_{12}}{dz},$$

where n = 1, 2 are the indices of the inductor and armature windings, respectively; v_z is the speed of movement of the armature winding along the z-axis.

Initial conditions of the mathematical model:
$i_n(0) = 0$ – current of the n-th winding;
$h_z(0) = z_0$ – armature winding displacement;
$T_n(0) = T_0$ – temperature of the n-th winding;
$u_c(0) = U_0$ – CES voltage;
$u(0) = U_\text{m} \sin\psi_u$ – AVS voltage;
$v_z(0) = 0$ – armature winding speed along the z-axis,
where U_m – voltage amplitude;
ψ_u=0 – initial phase of AVS voltage.

The mathematical model of the electromagnetic processes of the EIA at excitation from the CES is presented in [17], and at excitation from the AVS – in [18]. The mechanical processes of the accelerator take into account the masses of the armature winding and the actuator, the instantaneous position of the armature winding, the electrodynamic force between the windings and the aerodynamic resistance of the air environment [15]. The thermal processes of the accelerator take into account the specific heat, thermal conductivity, material density, specific resistance and current density j_n of the windings. Boundary conditions of the third kind are used on the cooling surfaces of the windings, and boundary conditions of the second kind are used on the axis of symmetry [19].

The amplitudes of the current densities in the windings of the inductor j_{1m} and of the armature j_{2m}, the amplitude of the electrodynamic force between the windings f_{zm}, the highest value of the armature speed v_{zm}, the speed of the armature at the output of the accelerator v_{zf}, when the electromagnetic processes decay, and the temperature rise of the inductor winding θ_1 and the armature winding θ_2 are used as the main indicators of the EIA.

EIA parameters. Consider an electromechanical accelerator with the following parameters: the inductor winding has an outer diameter D_{1ex} = 39 mm, an inner diameter D_{1in} = 27 mm, an axial height H_1 = 45 mm, and the number of turns N_1 = 120; the armature winding has an outer diameter D_{2ex} = 26 mm, an inner diameter D_{2in} = 20 mm, an axial height H_2 = 30 mm, and the number of turns N_2 = 40. The windings are wound with a round copper wire with a diameter of d_0 = 1.3 mm.

The CES has an energy of W_0 = 625 J and is implemented in two versions. Option I of the CES – charging voltage U_0 = 500 V and capacitance C_0 = 5000 μF and option II of the CES – U_0 = 707 V, C_0 = 2500 μF, which provide different duration of electrical processes.

The alternating voltage source has a voltage amplitude U_m = 100 V at frequencies of 50, 250 and 500 Hz and is connected to the inductor winding for a short time (t = 45 ms).

Let us consider the influence of the initial displacement z_0 of the armature winding relative to the inductor winding on the characteristics of the EIA of a cylindrical configuration. Note that for an accelerator with the specified geometrical parameters, the greatest value of the gradient of mutual inductance dM_{12}/dz occurs at z_{0m}≈10 mm (Fig. 1).

EIA indicators when excited from a capacitive energy storage. Let us consider the characteristics of the accelerator in the absence of an initial displacement (z_0 = 0), at a maximum displacement (z_0 = 20 mm) and at an intermediate displacement, in which the highest armature speeds at the output of the accelerator v_{zf} are provided.

The currents in the EIA windings have a vibration-damping character (Fig. 2,*a*).

When using the CES option I, the largest amplitude of the current density in the inductor winding j_{1m}= = 1.12 kA/mm^2 occurs at the maximum initial displacement, but the amplitude of the current density in the armature winding is the smallest – j_{2m}=0.2 kA/mm^2. The largest value of the current density – j_{2m}=1.4 kA/mm^2 occurs in the absence of an initial displacement. Note that for any initial displacement z_0, the currents in the windings practically decay after 10 ms.

The electrodynamic force f_z between the windings has an initial accelerating (positive) and subsequent braking (negative) components (Fig. 2,*b*). The accelerating component of the force arises at opposite polarities of the currents in the windings, and the braking one – at the same polarities of the currents. With an intermediate initial displacement z_0 = 8 mm, the amplitude of the accelerating component of the force is f_{zm} = 1.64 kN. Due to this pattern of changes in the electrodynamic force, the speed of the armature first

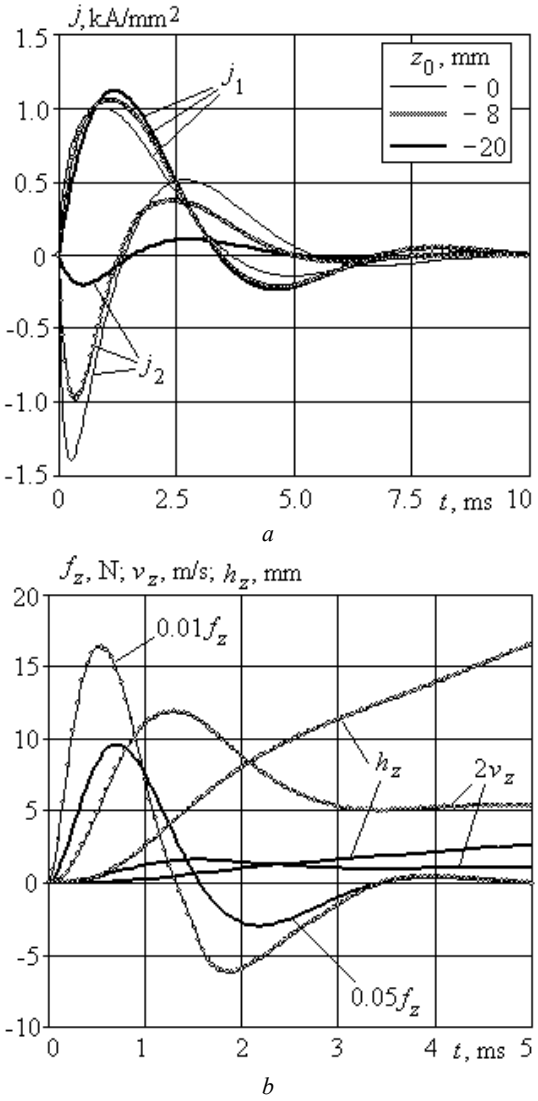

Fig. 2. Electrical (*a*) and mechanical (*b*) characteristics of the EIA at C_0=5000 μF, U_0=500 V

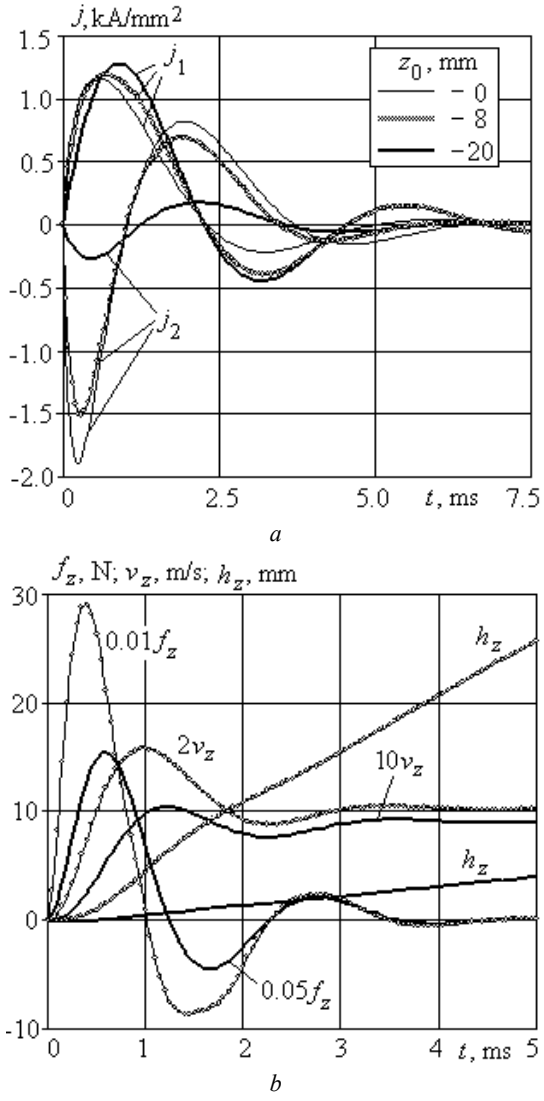

Fig. 3. Electrical (*a*) and mechanical (*b*) characteristics of the EIA at C_0=2500 μF, U_0=707 V

increases to a maximum value v_{zm} = 5.94 m/s, and then decreases by 2.23 times by the end of the electromagnetic process. The displacement of the armature winding h_z nonlinearly increases with time in the active section of acceleration, in which the electrodynamic interaction between the windings occurs. Obviously, the value of displacement h_z is significantly higher at the initial displacement of the windings z_0 = 8 mm than at z_0 = 20 mm. At z_0 = 0 mm, the mechanical indicators of the EIA of the cylindrical configuration are equal to zero. At z_0 = 8 mm, the temperature rise of the inductor winding is θ_1 = 6.3 K, and the temperature rise of the armature winding – θ_2 = 2.4 K.

When using the CES option II, the amplitudes of the current densities in the windings of the EIA increase (Fig. 3,*a*). The largest amplitude of the current density in the inductor winding occurs at the maximum initial displacement z_0 = 20 mm and is j_{1m}=1.28 kA/mm^2. The amplitude of the current density in the armature winding is minimal and amounts to j_{2m}=0.26 A/mm^2. In the absence of displacement (z_0 = 0 mm), the current density in the armature winding is maximum and is j_{2m}= 1.9 kA/mm^2.

The electrodynamic force f_z between the windings also has an initial accelerating and subsequent braking components (Fig. 3,*b*). With an intermediate initial displacement of the windings (z_0 = 6 mm), the amplitude of the accelerating component of the force increases to 2.9 kN. The armature winding speed initially increases to a maximum value of v_{zm} = 7.91 m/s, and then decreases by 1.54 times by the end of the electromagnetic process. At z_0 = 6 mm the temperature rise of the inductor winding is θ_1 = 5.9 K, and the temperature rise of the armature winding – θ_2 = 5.0 K.

Thus, in spite of the shorter force action, the use of a CES with a reduced capacity C_0 and an increased voltage U_0 provides higher speed indicators of an EIA of a cylindrical configuration. However, this is realized with different initial displacement of the windings z_0.

Figure 4 allows to estimate the influence of the initial displacement of the armature winding z_0 on the indicators of the accelerator, excited from the CES. Regardless of the option of the CES, the main dependencies of the EIA are as follows. When using the CES option I and increasing z_0 from 0 to 20 mm, the amplitude of the current density in the inductor winding

increases insignificantly (by 11.2 %), and in the armature winding decreases significantly (6.98 times). As a result, the temperature rise of the inductor winding increases by 19.1 %, and the temperature rise of the armature winding decreases by 32.1 times. However, the amplitude of the electrodynamic force f_{zm} and the speed at the output of the accelerator v_{zf} have pronounced maxima depending on the initial displacement of the windings z_0. The greatest amplitude of the force f_{zm} = 1.72 kN occurs at z_0≈6 mm, and the highest speed v_{zf} = 2.66 m/s – at z_0≈8 mm.

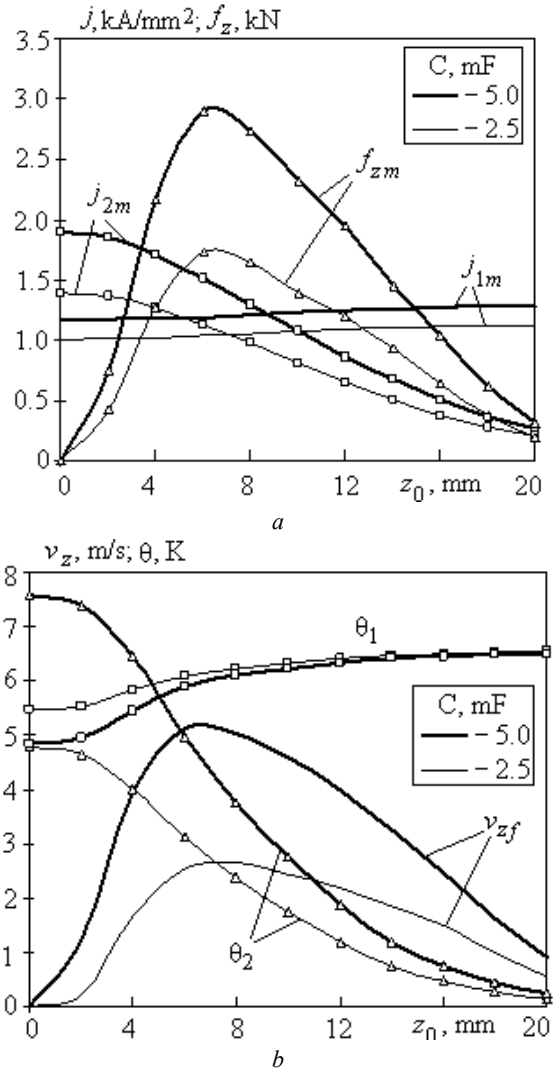

Fig. 4. Dependence of EIA indicators on the initial displacement of the windings when excited from the CES

When the EIA is excited from the CES option II, the amplitudes of the current densities in the windings increase, as do the rises of their temperatures. However, the highest speed v_{zf} = 5.11 m/s takes place at z_0≈6.5 mm.

EIA indicators when excited from an alternating voltage source. Let us consider the excitation of an EIA of a cylindrical configuration when excited from an alternating voltage source. If the AVS has a frequency ν=50 Hz, then a significant phase shift occurs between the currents in the windings at an initial displacement z_0 = 6 mm, leading to the appearance of alternating accelerating and braking components of electrodynamic forces (Fig. 5).

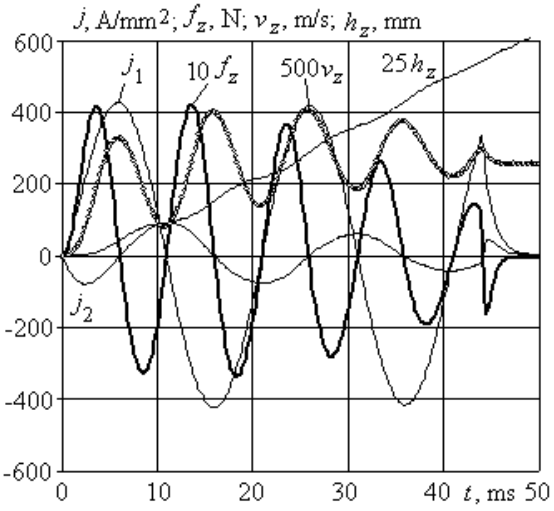

Fig. 5. Electromechanical indicators of the EIA at excitation from the AVS with frequency of 50 Hz at z_0=6 mm

Since the accelerating components of the force prevail over the braking components, the armature winding moves relative to the inductor winding by a distance h_z at a speed v_{zf} = 0.51 m/s. At such a frequency of the AVS, the current amplitude in the armature winding is about 4 times less than in the inductor winding. Moreover, the current density in the armature winding decreases as it moves relative to the inductor winding.

Since the phase shift between the winding currents decreases with an increase in the AVS frequency, the braking component of the electrodynamic force also decreases accordingly. Figure 6 shows the electromechanical indicators of the accelerator at excitation from the AVS with a frequency of 250 Hz at z_0 = 8 mm. With this excitation, in comparison with excitation with a frequency of 50 Hz, the current in the inductor winding decreases, and in the armature winding it increases. In the initial period of excitation, the current densities in the windings are comparable. However, due to a decrease in the magnetic coupling between the windings, the current density in the inductor winding reaches a steady-state value, and in the armature winding it almost completely decays by the end of the excitation period.

But due to the greater displacement of the armature winding relative to the inductor winding, for the same time the magnetic coupling decreases faster, which leads to a stronger damping of the electrodynamic force. This force decays after almost 30 ms. Its accelerating components increase, while the braking ones decrease, which leads to a higher speed at the output of the accelerator v_{zf} =1.9 m/s than at an AVS frequency of 50 Hz.

At the maximum initial displacement between the windings (z_0 = 20 mm), the following changes occur in the electromechanical processes (Fig. 7). With a practically unchanged current density in the inductor winding j_1, the current density in the armature winding j_2 at the initial stage significantly decreases due to the weakened magnetic coupling. However, over time, the current in the armature winding and the electrodynamic

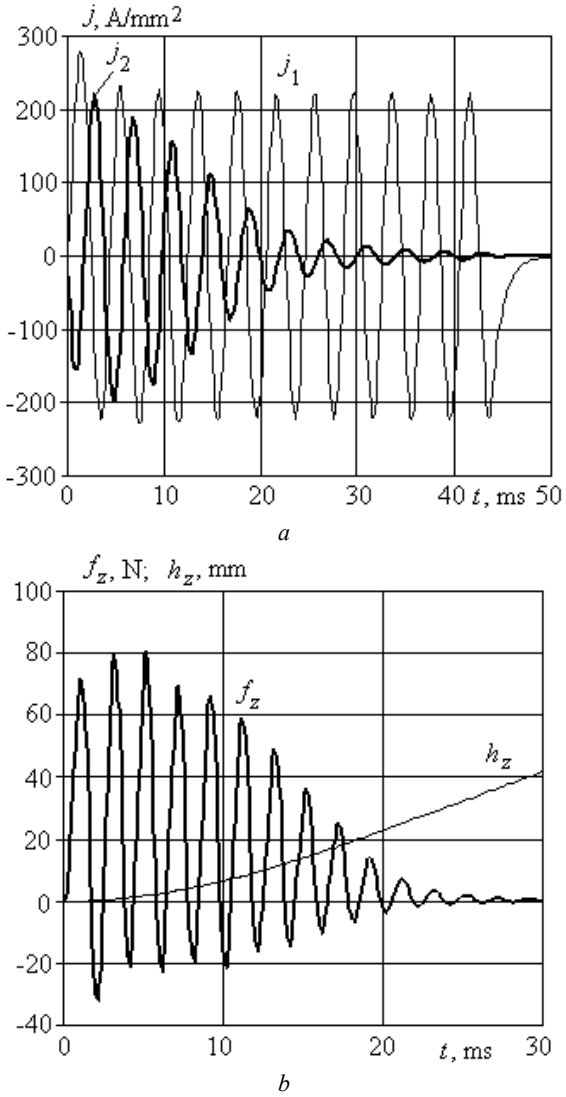

Fig. 6. Electromechanical indicators of the EIA at excitation from the AVS with frequency of 250 Hz at z_0=8 mm

force decay at a lower rate. This is due to the fact that due to the reduced speed v_z, the armature moves a smaller distance relative to the inductor winding.

With an increase in the AVS frequency to 500 Hz, the ratio between the amplitudes of the currents in the windings at the initial stage changes (Fig. 8). The value of the current density in the armature winding exceeds the same value in the inductor winding. In this case, the phase shift between the windings is further reduced. As a result, the braking components of the electrodynamic force decrease, which leads to an increase in the armature speed at the output of the accelerator to v_{zf} = 2.2 m/s, despite a decrease in the accelerating components of the force.

Figure 9 makes it possible to estimate the influence of the initial displacement of the armature winding on the indicators of the EIA of a cylindrical configuration when excited from the AVS.

With an increase in the initial displacement of the armature winding z_0 from 0 to 20 mm, the maximum speed at the output of the accelerator strongly depends on the AVS frequency.

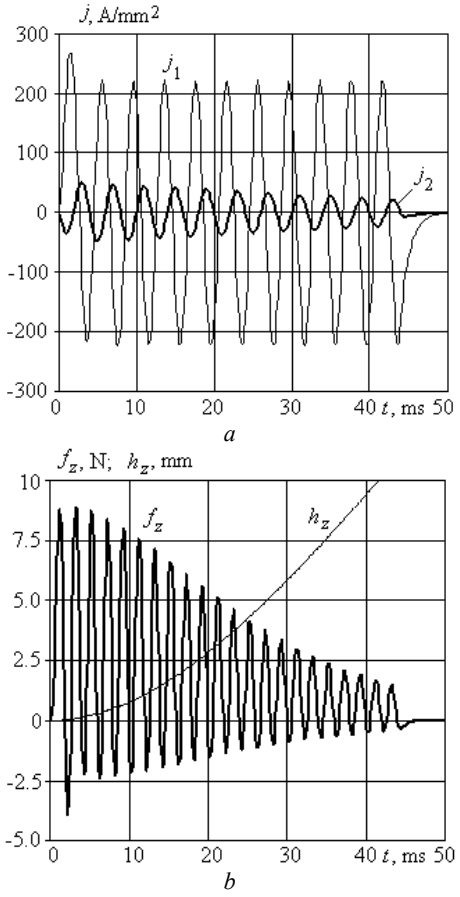

Fig. 7. Electromechanical indicators of the EIA at excitation from the AVS with frequency of 250 Hz at z_0=20 mm

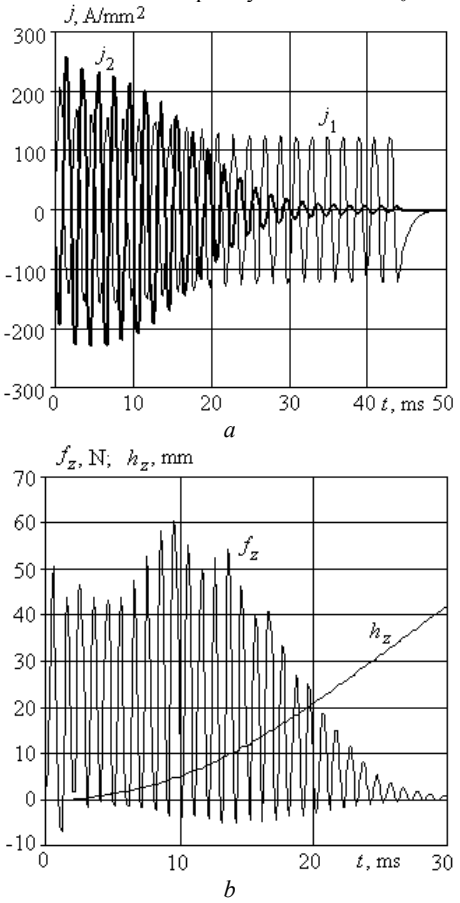

Fig. 8. Electromechanical indicators of the EIA at excitation from the AVS with frequency of 500 Hz at z_0=4 mm

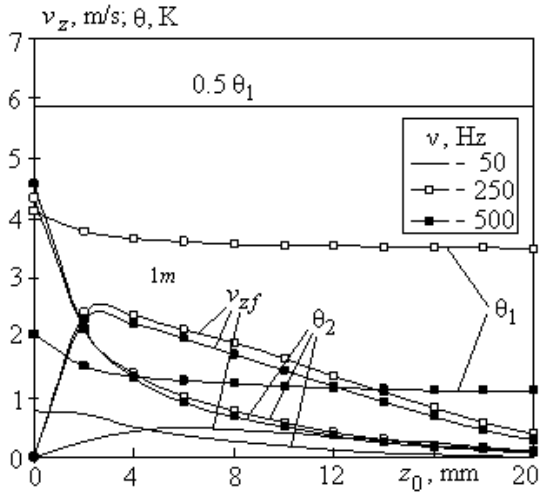

Fig. 9. Dependence of EIA indicators on the initial displacement of the windings when excited from the AVS

At a frequency of 50 Hz, the highest speed at the accelerator output v_{zf} = 0.5 m/s is realized at z_0 = 6.2 mm, at a frequency of 250 Hz – v_{zf} = 2.4 m/s at z_0 = 3.1 mm, and at a frequency of 500 Hz – v_{zf} = 2.29 m/s at z_0 = 2.3 mm. With an increase in the AVS frequency, the temperature rise of the inductor winding θ_1 decreases, and the temperature rise of the armature winding θ_2 increases.

At a frequency of 50 Hz, the value of θ_1 is practically independent on the initial displacement of the windings. However, at higher frequencies, with an increase in the initial displacement, the value θ_1 slightly decreases. The temperature rise of the armature winding θ_2 decreases to a greater extent from the value of z_0 in comparison with the temperature rise of the inductor winding.

Thus, when the EIA is excited from the CES, the initial displacement of the windings should be approximately $z_0 \approx 0.6 z_{0m}$, where z_{0m} is the distance at which the largest dM_{12}/dz value between the windings is ensured. When the EIA is excited from the AVS, the initial displacement z_0 must be selected depending on its frequency: at a frequency of 50 Hz – $z_0 \approx 0.6 z_{0m}$, and at frequencies of 250 Hz and 500 Hz – $z_0 \approx 0.2 z_{0m}$.

Conclusions.

When a cylindrical EIA is excited, the largest amplitude of the current density in the inductor winding occurs at the maximum initial displacement, but the amplitude of the current density in the armature winding is the smallest. The greatest value of the current density in the armature winding occurs in the absence of an initial displacement.

When excited from the CES, the electrodynamic force between the windings has an initial accelerating and subsequent braking components. As a result, the speed of the armature initially increases to a maximum value, but decreases towards the end of the electromagnetic process.

When a cylindrical EIA is excited from the AVS, a phase shift occurs between the currents in the windings, which leads to the appearance of alternating accelerating and breaking components of electrodynamic forces. The accelerating components of the force prevail over the braking components which ensures the displacement of the armature.

At an AVS frequency of 50 Hz, the current amplitude in the armature winding is less than in the inductor winding. With an increase in the AVS frequency to 250 Hz, the phase shift between the winding currents decreases. The current in the inductor winding decreases, and in the armature winding it increases. The accelerating components of the force increase, and the braking ones decrease. With an increase in the AVS frequency to 500 Hz, the value of the current density in the armature winding exceeds the same value in the inductor winding. In this case, the phase shift between the windings is further reduced.

At an AVS frequency of 50 Hz, the highest speed v_{zf} = 0.5 m/s is realized at the initial displacement of the windings z_0 = 6.2 mm, at a frequency of 250 Hz the highest speed v_{zf} = 2.4 m/s is realized at z_0 = 3.1 mm, and at a frequency of 500 Hz, the highest speed v_{zf} = 2.29 m/s is realized at z_0 = 2.3 mm.

Conflict of interest. The authors declare that they have no conflicts of interest.

REFERENCES

1. Guangcheng F., Wang Y., Xu Q., Xinyi N., Yan Z. Design and analysis of a novel three-coil reconnection electromagnetic launcher. *IEEE Transactions on Plasma Science*, 2019, vol. 47, no. 1, pp. 814-820. doi: https://doi.org/10.1109/tps.2018.2874287.

2. Puumala V., Kettunen L. Electromagnetic design of ultrafast electromechanical switches. *IEEE Transactions on Power Delivery*, 2015, vol. 30, no. 3, pp. 1104-1109. doi: https://doi.org/10.1109/tpwrd.2014.2362996.

3. Kostsov E.G. Microelectromechanical accelerator of solids. *Optoelectronics, Instrumentation and Data Processing*, 2012, no. 48, pp. 401-409. doi: https://doi.org/10.3103/S8756699012040115.

4. Reck B. First design study of an electrical catapult for unmanned air vehicles in the several hundred kilogram range. *IEEE Transactions on Magnetics*, 2003, vol. 39, no. 1, pp. 310-313. doi: https://doi.org/10.1109/tmag.2002.805921.

5. Chemeris V.T. Multistage induction accelerator of a macro-object: search for technical solutions. *Artillery and small arms*, 2011, no. 3 (40), pp. 45-51. (Rus).

6. Bolyukh V.F., Shchukin I.S. *Lineinye induktsionno-dinamicheskie preobrazovateli* [Linear induction-dynamic converters]. Saarbrucken, Germany, LAP Lambert Academic Publ., 2014. 496 p. (Rus).

7. Novakovic Z., Vasic Z., Ilic I., Medar N., Stevanovic D. Integration of tactical - medium range UAV and catapult launch system. *Scientific Technical Review*, 2016, vol. 66, no. 4, pp. 22-28. doi: https://doi.org/10.5937/str1604022n.

8. Angquist L., Baudoin A., Norrga S., Nee S., Modeer T. Low-cost ultra-fast DC circuit-breaker: Power electronics integrated with mechanical switchgear. *2018 IEEE International Conference on Industrial Technology (ICIT)*, 2018, pp. 1708-1713. doi: https://doi.org/10.1109/icit.2018.8352439.

9. Gerasimov Yu.V., Karetnikov G.K., Selivanov A.B., Fionov A.S. Evaluation of relative final mass of a nanosatellite delivered to the near-earth space using a pulsed launcher and a pulsed correcting thruster. *Herald of the Bauman Moscow State Technical University. Series Mechanical Engineering*, 2013, no. 3 (92), pp. 69-76. (Rus). Available at: http://vestnikmach.ru/articles/116/eng/116.pdf (accessed 15 May 2021).

10. Upshaw J.L., Kajs J.P. Micrometeoroid impact simulations using a railgun electromagnetic accelerator. *IEEE Transactions on Magnetics*, 1991, vol. 27, no. 1, pp. 607-610. doi: https://doi.org/10.1109/20.101103.

11. Bissal A. *On the design of ultra-fast electro-mechanical actuators. Licentiate Thesis*. Stockholm, Sweden, 2013. 76 p.

Available at: https://www.diva-portal.org/smash/get/diva2:617236/FULLTEXT01.pdf (accessed 15 May 2021).
12. Torlin V.N. Vetrogon A.A., Ogryzkov S.V. Behavior of electronic units and devices under the influence of shock loads in an accident, *Automobile transport*, 2009, vol. 25, pp. 178-180. (Rus). Available at: https://dspace.khadi.kharkov.ua/dspace/bitstream/123456789/807/1/39.pdf (accessed 15 May 2021).
13. Kondratiuk M., Ambroziak L. Concept of the magnetic launcher for medium class unmanned aerial vehicles designed on the basis of numerical calculations, *Journal of Theoretical and Applied Mechanics*, 2016, vol. 54, no. 1, pp. 163-177. doi: https://doi.org/10.15632/jtam-pl.54.1.163.
14. Li S., Gui Y., Yu C., Liu P., Zhang P., Li J. Study on the effect and the direction accuracy of active electromagnetic protection system. *IEEE Transactions on Magnetics*, 2009, vol. 45, no. 1, pp. 351-353. doi: https://doi.org/10.1109/TMAG.2008.2008850.
15. Bolyukh V.F., Oleksenko S.V., Schukin I.S. Efficiency of linear pulse electromechanical converters designed to create impact loads and high speeds. *Electrical Engineering & Electromechanics*, 2015, no. 3, pp. 31-40. doi: https://doi.org/10.20998/2074-272X.2015.3.05.
16. Bolyukh V.F., Shchukin I.S. Influence of an excitation source on the power indicators of a linear pulse electromechanical converter of induction type. *Technical Electrodynamics*, 2021, no. 3, pp. 28-36. doi: https://doi.org/10.15407/techned2021.03.028.
17. Bolyukh V.F., Katkov I.I. Influence of the Form of Pulse of Excitation on the Speed and Power Parameters of the Linear Pulse Electromechanical Converter of the Induction Type. *Volume 2B: Advanced Manufacturing*, Nov. 2019, 8 p. doi: https://doi.org/10.1115/imece2019-10388.
18. Bolyukh V.F., Kashansky Yu.V., Schukin I.S. Features of excitation of a linear electromechanical converter of induction type from an AC source. *Electrical Engineering & Electromechanics*, 2021, no. 1, pp. 3-9. doi: https://doi.org/10.20998/2074-272x.2021.1.01.
19. Bolyukh V.F., Shchukin I.S. The thermal state of an electromechanical induction converter with impact action in the cyclic operation mode, *Russian Electrical Engineering*, 2012, vol. 83, no. 10, pp. 571-576. doi: https://doi.org/10.3103/S1068371212100045.

Received 10.07.2021
Accepted 25.09.2020
Published 26.10.2021

V.F. Bolyukh[1], *Doctor of Technical Science, Professor,*
I.S. Schukin[2], *PhD, Associate Professor,*
J. Lasocki [3], *PhD, Associate Professor,*
[1] National Technical University «Kharkiv Polytechnic Institute»,
2, Kyrpychova Str., Kharkiv, 61002, Ukraine,
e-mail: vfbolyukh@gmail.com (Corresponding author)
[2] Firm Tetra, LTD,
18, Gudanova Str., Kharkiv, 61024, Ukraine,
e-mail: tech@tetra.kharkiv.com.ua
[3] Warsaw University of Technology,
Narbutta 84, 02-524, Warsaw, Poland,
e-mail: jakub.lasocki@pw.edu.pl

How to cite this article:
Bolyukh V.F., Schukin I.S., Lasocki J. Influence of the initial winding displacement on the indicators of the electromechanical induction accelerator of cylindrical configuration. *Electrical Engineering & Electromechanics*, 2021, no. 5, pp. 3-10. doi: https://doi.org/10.20998/2074-272X.2021.5.01.